

RESEARCH ARTICLE

Inverse Eigenvalue Difference Problems for Quantum Dots

¹Department Applied Mathematics, University of California, Merced, California, USA | ²Department of Physics, University of California, Merced, California, USA

Correspondence: Kyle Wright (kwright11@ucmerced.edu)

Received: 4 October 2024 | Revised: 6 March 2025 | Accepted: 14 April 2025

Funding: This work was supported by the NSF, Grant/Award Numbers: DGE2125510; DMS1840265

Keywords: characteristic polynomial | least-squares | optimization | quantum sensing

ABSTRACT

A system of three tunnel-coupled quantum dots is considered in the presence of an applied electric field. Given the measurements of differences between ground state energy levels as the electric field is varied, we seek to recover the quantum Hamiltonian matrix that describes this system. We formulate this as an inverse Eigenvalue difference problem and develop algebraic and computational methods along with a warm starting strategy to solve it. The results demonstrate the efficacy of these approaches in the presence of measurement noise.

1 | Introduction

Inverse eigenvalue difference problems (IEPs) arise in many branches of science and engineering [1-4]. Broadly speaking, IEPs involve reconstructing a matrix from its eigenvalues. The breadth of IEPs has been expanding with scientific and technological progress. In this vein, this study describes an IEP that arises in the emerging field of quantum sensing, which facilitates high-resolution sensing of gravitation, acoustic waves, and electromagnetic fields [5-14]. We study a system of coupled quantum dots (QDs). The eigenstates of coupled quantum dot systems, such as self-assembled epitaxial quantum dots, can be experimentally measured primarily through optical techniques. These methods rely on the interaction of light with the quantum dot system, providing direct access to energy levels and transitions between them. Among the most widely used techniques are emission spectroscopy, including photoluminescence (PL) and photoluminescence excitation (PLE), as well as laser spectroscopy methods such as differential transmission, reflection, and absorption measurements [12, 13, 15-20].

In laser spectroscopy, a tunable laser excites electrons from the valence band to the conduction band of the quantum dots, creating holes in the valence band. The optical response—measured as variations in transmitted, reflected, or absorbed laser intensity—maps the allowed transitions between quantum dot eigenstates as a function of photon energy. In PL and PLE, the system is excited, and the emitted photons are detected as electrons recombine with holes. PL typically involves non-resonant or quasi-resonant excitation, where the electron first relaxes to lower-energy conduction band states via phonon interactions before recombining with a hole, emitting a photon. Because phonon-mediated relaxation is non-deterministic, PL spectra provide insight into a range of accessible states. In PLE, instead of measuring all emitted photons, the intensity of a specific emission line is monitored as a function of excitation wavelength, offering spectral information similar to laser spectroscopy.

If the quantum dots are integrated into tunable electric field environments, such as Schottky-type or p-i-n diode structures, their optical spectra can be measured as a function of applied electric field. This allows experimental observation of energy shifts due to potential variations and the quantum-confined Stark effect [12, 14, 21]. In coupled quantum dot systems, applying an electric

© 2025 John Wiley & Sons Ltd.

field enables control over eigenstate alignment, facilitating electron or hole tunneling between neighboring dots [17, 22]. These tunneling processes manifest in optical spectra as avoided crossings, revealing the underlying structure of electron or hole energy levels. By systematically analyzing these crossings, one can reconstruct the energy landscape of the system [23].

The energy levels of the QDs are represented by a quantum Hamiltonian matrix. The matrix elements depend on intrinsic physical properties, such as polarizabilities, spin-orbit coupling, and quantum tunneling, which, in turn, can reveal useful data about the system, such as the distances between the QDs. However, measuring this data directly is challenging. Thus, the objective is to determine the matrix elements from spectral measurements, forming an IEP.

There are many categorizations of IEPs. The primary IEP categorizations of interest to us are structured [24], parameterized [25], and partially described [26, 27]. Structured IEPs impose some structure on the recovered matrix. This could include requiring the matrix to be symmetric, tridiagonal, orthogonal, or nonnegative. In this case, structure is imposed by requiring the matrix to be symmetric, tunnel coupling is negligible between two quantum dots due to sufficient distance between quantum dots, and the structural dependence on electric field is assumed to be known. In this work, we define Parameterized IEPs as an IEP involving one or more elements of the matrix to be functions of a known, tunable parameter. In our case, this appears from the diagonal elements being function of an applied electric field. Partially described IEPs occur when the full spectral information of the matrix is unknown. Using eigenvalue differences instead of eigenvalues classifies this problem as a partially described IEP. The IEP studied in this paper is an overlap of these three categorizations.

Mathematically, our IEP differs from those that have been studied in two significant ways.

- 1. The matrix depends on a "tunable" (known) parameter. Specifically, the diagonal elements are quadratic polynomials of an applied electric field [28, 29]. As this field is varied between measurements, so does the matrix. Thus, this is a one-parameter family of matrices. In our terminology, the parameter (electric field) is known—its values are selected during measurements, whereas the polynomials' coefficients are unknown.
- 2. The eigenvalue *differences* are measured for a set of electric field values, but the eigenvalues themselves are unknown. The physical reason for this is that, as the QDs transition between energy states, they emit photons whose frequencies are proportional to energy differences. These photons are measured using photoluminescence techniques. We refer to this as an Inverse Eigenvalue Difference Problem (IEDP).

To the best of our knowledge, IEPs of this kind have not received attention. We develop a combination of analytical and computational methods to solve this IEDP. A common strategy for solving IEPs numerically is constructing a system of equations satisfied by the Hamiltonian and implementing a Newton method [30–32]. We build upon this framework and previous work

solving IEDPs for 2×2 matrices [29], exploring two formulations converting an IEP to an IEDP and a warmstarting approach to help ensure the initial iterate is sufficiently close for a Newton method to converge.

2 | Problem Description

We consider a system of three QDs, whose ground-state quantum Hamiltonian is, in general, described by a 3×3 real symmetric matrix [28] of the form

$$G(F) = \begin{bmatrix} g_1(F) & y_0 & y_1 \\ y_0 & g_2(F) & y_2 \\ y_1 & y_2 & g_3(F) \end{bmatrix}.$$
 (1)

Here, the diagonal elements correspond to the self-energies of each QD, whereas, the off-diagonal elements correspond to tunnel-coupling energies between the QDs. We further assume that the diagonal elements depend quadratically on the applied electric field, $F \in \mathbb{R}$, as

$$g_i(F) = \alpha_i + \beta_i F + \gamma_i F^2, \quad i = 1, 2, 3,$$
 (2)

where the coefficients $\{\alpha_i, \beta_i, \gamma_i\}$ are real. Equation (2) models the quadratic Stark shift [33]. The coefficients α_i are the eigenenergies absent an electric field. The coefficients β_i are the electric dipole moments, which are proportional to the distances between the QDs. The coefficients γ_i correspond to the polarizabilities of the ground-state electronic and hole wavefunctions. The off-diagonal elements correspond to hole tunneling strengths. The (implied) assumption that the off-diagonal elements are independent of F is a good approximation for weak electric fields and for weak tunnel-coupling between the QDs.

In this work, we consider a specific physical system. In particular, we assume that $y_1 = y_0$, which roughly corresponds to a system where the three QDs are similar and equally spaced on a straight line. In addition, we assume that $y_2 = 0$, which means that the QDs are far apart. Therefore, we have the Hamiltonian matrix

$$G(F) = \begin{bmatrix} {}^{\iota}g_{1}(F) & y_{0} & y_{0} \\ y_{0} & g_{2}(F) & 0 \\ y_{0} & 0 & g_{3}(F) \end{bmatrix}.$$
 (3)

Since G(F) is symmetric, its eigenvalues are real. We denote its eigenvalues by $\{\xi_1(F), \xi_2(F), \xi_3(F)\}$. The physical measurements can be used to determine the *differences* between the eigenvalues of G(F). The eigenvalue differences are denoted by

$$D_{2,1}(F) \equiv \xi_2(F) - \xi_1(F),$$
 (4)

$$D_{3,1}(F) \equiv \xi_3(F) - \xi_1(F), \tag{5}$$

$$D_{3,2}(F) \equiv \xi_3(F) - \xi_2(F). \tag{6}$$

Note that $D_{3,2}(F)=D_{3,1}(F)-D_{2,1}(F)$. The measured data is provided over a set of n values of $F\in\mathbb{R}$, denoted by $\{F_k\}_{k=1}^n$. Hence, we consider the measured dataset to be

$$M = \left\{ F_k, D_{2,1}(F_k), D_{3,1}(F_k) \right\}_{k=1}^n \tag{7}$$

Our objective is to recover G(F) using the dataset M. In Appendix A we prove that, without loss of generality, one can set $g_1(F) = 0$. This has the effect of eliminating an arbitrary shift in the diagonal elements and in the eigenvalues of G(F) that would satisfy the dataset M. For this reason, henceforth we consider

$$G(F) = \begin{bmatrix} 0 & y_0 & y_0 \\ y_0 & g_2(F) & 0 \\ y_0 & 0 & g_3(F) \end{bmatrix}.$$
 (8)

We denote the vector of unknown coefficients as (for convenience we also refer to y_0 as a coefficient)

$$\mathbf{p} = [y_0, \alpha_2, \beta_2, \gamma_2, \alpha_3, \beta_3, \gamma_3] \in \mathbb{R}^7$$
(9)

and denote the "ground truth" coefficients by \mathbf{p}^* , which corresponds to G(F) that generates the dataset M. We also use the more compact notation

$$\mathbf{p} = [y_0, \mathbf{p}_{g_\alpha}, \mathbf{p}_{g_\alpha}] \in \mathbb{R}^7 \tag{10}$$

where $\mathbf{p}_{g_i} = [\alpha_i, \beta_i, \gamma_i] \in \mathbb{R}^3$ for i = 2, 3. To summarize, we seek to solve the following:

Inverse Eigenvalue Difference Problem (IEDP)

Given the eigenvalue difference dataset M in (7), find coefficients \mathbf{p} , such that G(F) in (8) generates M.

For ease of presentation, we shall assume that the off-diagonal elements are positive, i.e., $y_0 > 0$, which corresponds to positive tunnel coupling. However, our methods still work if $y_0 \le 0$.

Importantly, in the presence of noisy data, a solution of this IEDP is understood as a solution of a related optimization problem (see Section 4.2). Though this IEDP does not have a unique solution, the diversity of the spectral data for the different values of F_k reduces the non-uniqueness. In particular, in Appendix B we prove the following:

Proposition 1. The IEDP with $n \ge 5$ values of F has at most four solutions. In particular, if $\mathbf{p}^* = [y_0^*, \mathbf{p}_{g_2}^*, \mathbf{p}_{g_3}^*]$ is a solution, then there are four solutions, which are

$$[y_0^*, \mathbf{p}_{g_2}^*, \mathbf{p}_{g_3}^*], \quad [y_0^*, \mathbf{p}_{g_3}^*. \mathbf{p}_{g_2}^*], \quad [y_0^*, -\mathbf{p}_{g_2}^*, -\mathbf{p}_{g_3}^*], \quad \text{and} \quad [y_0^*, -\mathbf{p}_{g_3}^*. -\mathbf{p}_{g_2}^*] \quad \text{(11)}$$

These solutions are different unless $g_2(F) = g_3(F)$, i.e., the diagonal elements are the same.

The four solutions in (11) correspond to the invariance of the eigenvalues to the swapping of the diagonal elements g_2 and g_3 and the nonuniqueness of eigenvalues resulting in eigenvalue differences. In this sense, we refer to "uniqueness" up to these four types of solutions.

3 | Previous Approach

In previous work, we developed an approach for solving the eigenvalue difference problem for a 2×2 G(F) matrix [29]. In

this section, we discuss this previous method, how it scales in higher dimensions, and our decision to formulate an alternative approach.

Consider the leading 2×2 matrix $G_2(F)$ of G(F) given by

$$G_2(F) = \begin{bmatrix} 0 & y \\ y & \alpha + \beta F \end{bmatrix},\tag{12}$$

where the coefficient of the quadratic term is 0. The eigenvalues of $G_2(F)$ are given explicitly by

$$\xi_1(F) = \frac{1}{2}(\alpha + \beta F) - \frac{1}{2}\sqrt{(\alpha + \beta F)^2 + 4y^2} \quad \text{and}$$

$$\xi_2(F) = \frac{1}{2}(\alpha + \beta F) + \frac{1}{2}\sqrt{(\alpha + \beta F)^2 + 4y^2}$$
 (13)

It follows from (4) and (13) that

$$[D_{2,1}(F)]^2 = \beta^2 F^2 + 2\alpha\beta F + \alpha^2 + 4y^2 \tag{14}$$

Assuming that the set $\{D_{2,1}(F)\}$ is known for (at least) three values of F, we can recover β , α , and y by solving the least-squares problem

$$\min_{\kappa_0, \kappa_1, \kappa_2} \sum_{k=1}^{n} \left\{ [D_{2,1}(F_k)]^2 - (\kappa_2 F_k^2 + \kappa_1 F_k + \kappa_0) \right\}^2$$
 (15)

and letting

$$\beta = \pm \sqrt{\kappa_2}$$
, $\alpha = \frac{\kappa_1}{2\beta}$, and $y = \frac{1}{2}\sqrt{\kappa_0 - \alpha^2}$ (16)

In our approach, we solve the normal equations associated with (15) to obtain κ_0 , κ_1 , and κ_2 .

The left- and right-hand sides of (14) are expressions of the discriminant of the characteristic polynomial of $G_2(F)$. In general, for any square matrix G, the left-hand side of (14) can be generalized as the product of the squared-differences between the eigenvalues, i.e.,

$$d(G) = \prod_{i \le j} (\lambda_i - \lambda_j)^2 \tag{17}$$

which is called the discriminant. It is well-known that the discriminant can be expressed in terms of the matrix elements as follows. Let G be an $m \times m$ matrix, $p_G(\lambda)$ its characteristic polynomial, and $p'_G(\lambda)$ its derivative with respect to λ . Let S be the $(2m-1)\times(2m-1)$ Sylvester matrix [34] associated with $p_G(\lambda)$ and $p'_G(\lambda)$. The determinant of S is the resultant of $p_G(\lambda)$ and $p'_G(\lambda)$, which can be shown to be the same as the discriminant [34, 35], i.e., (14) generalizes as

$$d(G) = \det(S(p_G(\lambda), p'_G(\lambda))).$$

It is possible to calculate $\det(S)$ using symbolic algebra algorithms and use this to generalize the above approach to any square matrix. However, this approach scales poorly as the size of G(F) increases. In particular, for an $m \times m$ matrix G(F), $\det(S)$ (and thus d(G)) is a homogeneous polynomial in the elements of G(F) of degree m(m-1) [34, 35]. Assuming the diagonal

elements of G(F) are degree-r polynomials in F, the discriminant is a polynomial in F of degree

$$\deg[d(G(F))] = m(m-1)r \tag{18}$$

with coefficients $\{\kappa_i\}_{i=1}^{1+m(m-1)r}$ that generalize the right-hand side of (14). Therefore, it would require at least 1+m(m-1)r equations to have unique κ 's, which implies that this approach requires at least 1+m(m-1)r data points of F. Once the κ coefficients have been found, the coefficients in G(F) (that generalize y, α, β above) can be found by solving a set of polynomial equations of degree m(m-1). While this could work, we propose an alternative approach that is lower-degree in the coefficients of G(F) and requires significantly fewer data points of F.

4 | Proposed Approach

In this section, we outline our proposed approach to recover the vector of coefficients \mathbf{p} in G(F). To do this, we algebraically derive a vector function whose root corresponds to the solution \mathbf{p}^* , and formulate an optimization problem using this vector function. Due to the importance of initial iterates when solving optimization problems for related IEPs [36], we also propose an approach for generating sufficiently good initial iterates.

For clarity of presentation, we suppress the dependence of the eigenvalues $\xi_i(F)$, the quadratic diagonal functions $g_i(F)$, and the eigenvalue differences $D_{i,j}(F)$ on F in this section.

4.1 | Algebraic Formulation

The eigenvalues of G(F) are roots of the characteristic polynomial

$$\det(G(F) - \xi I) = \zeta_0(\mathbf{p}) + \zeta_1(\mathbf{p})\xi + \zeta_2(\mathbf{p})\xi^2 - \xi^3 \tag{19}$$

where the coefficients are given by

$$\zeta_0(\mathbf{p}) = -(g_2 + g_3)y_0^2$$
, $\zeta_1(\mathbf{p}) = -(g_2g_3 - 2y_0^2)$, and $\zeta_2(\mathbf{p}) = g_2 + g_3$

Since the eigenvalues of G(F) are known to be roots of the characteristic polynomial, the characteristic polynomial is also given by

$$\det(G(F) - \xi I) = (\xi_1 - \xi)(\xi_2 - \xi)(\xi_3 - \xi) \tag{21}$$

Comparing the coefficients in (19) with those in (21) leads to the following system of equations:

$$\tilde{\mathcal{F}}_{0}(\mathbf{p}, \xi_{1}, \xi_{2}, \xi_{3}) = \zeta_{0}(\mathbf{p}) - \xi_{1}\xi_{2}\xi_{3} = 0$$
 (22a)

$$\tilde{\mathcal{F}}_{1}(\mathbf{p}, \xi_{1}, \xi_{2}, \xi_{3}) = \zeta_{1}(\mathbf{p}) + (\xi_{1}\xi_{2} + \xi_{1}\xi_{3} + \xi_{2}\xi_{3}) = 0$$
 (22b)

$$\tilde{\mathcal{F}}_{2}(\mathbf{p}, \xi_{1}, \xi_{2}, \xi_{3}) = \zeta_{2}(\mathbf{p}) - (\xi_{1} + \xi_{2} + \xi_{3}) = 0$$
 (22c)

whose solution is \mathbf{p}^* . We can eliminate ξ_2 and ξ_3 from these functions using the eigenvalue differences $D_{2,1}$ and $D_{3,1}$ from (4) and (5), respectively, yielding the following system of equations:

$$\mathcal{F}_0(\mathbf{p},\xi_1) = -(g_2+g_3)y_0^2 - \xi_1(\xi_1+D_{2,1})(\xi_1+D_{3,1}) = 0 \; , \eqno(23)$$

$$\mathcal{F}_1(\mathbf{p}, \xi_1) = g_2 g_3 - 2y_0^2 - \xi_1(\xi_1 + D_{2,1}) - \xi_1(\xi_1 + D_{3,1}) - (\xi_1 + D_{2,1})(\xi_1 + D_{3,1}) = 0,$$
(24)

$$\mathcal{F}_2(\mathbf{p},\xi_1) = g_2 + g_3 - \xi_1 - (\xi_1 + D_{2,1}) - (\xi_1 + D_{3,1}) = 0 \; , \eqno(25)$$

which contains the seven unknown coefficients in **p**. We note that, at this point, ξ_1 is also unknown since our data consist only of the eigenvalue differences $D_{2,1}$ and $D_{3,1}$ at each F_k .

Formulation I: We can eliminate ξ_1 in (23) and (24) by first defining the function

$$\psi(\mathbf{p}_{g_2}, \mathbf{p}_{g_3}) = \frac{1}{3}(g_2 + g_3 - D_{2,1} - D_{3,1}).$$
 (26)

Note that at the true coefficients $\mathbf{p}_{g_2}^*$ and $\mathbf{p}_{g_3}^*$, we have that $\psi(\mathbf{p}_{g_2}^*,\mathbf{p}_{g_3}^*)=\xi_1$ from (25). Then, substituting ψ in (23) and (24) gives the system of equations

$$\mathcal{F}_0^{(I)}(\mathbf{p}) = -(g_2 + g_3)y_0^2 - \psi(\psi + D_{2,1})(\psi + D_{3,1}) = 0 \quad (27a)$$

$$\mathcal{F}_{1}^{(I)}(\mathbf{p}) = g_{2}g_{3} - 2y_{0}^{2} - \psi(\psi + D_{2,1}) - \psi(\psi + D_{3,1})$$
$$-(\psi + D_{2,1})(\psi + D_{3,1}) = 0$$
(27b)

According to Proposition 1, n = 5 values of F are sufficient to guarantee a unique solution. By choosing n = 5 values of F, we get 10 equations from (27) in the 7 unknowns.

Formulation II: In this formulation, we eliminate the coefficient y_0 . We define a new function

$$\phi(\mathbf{p}_{g_2}, \mathbf{p}_{g_3}; F) = \frac{1}{2} \left(g_2 g_3 - D_{2,1} D_{3,1} \right) + \frac{1}{6} \left((D_{2,1} + D_{3,1})^2 - (g_2 + g_3)^2 \right), \tag{28}$$

where we explicitly show the dependence of ϕ on F. The motivation for this definition is as follows: By substituting (26) into (27b), at the true coefficients $\mathbf{p}_{g_3}^*$ and $\mathbf{p}_{g_3}^*$, it follows that

$$\phi(\mathbf{p}_{g_2}^*, \mathbf{p}_{g_3}^*; F) = y_0^2 \tag{29}$$

for all F. We substitute ϕ in (27a) to obtain a new equation,

$$\mathcal{F}_0^{(II)}(\mathbf{p}_{g_2}, \mathbf{p}_{g_3}) = -(g_2 + g_3)\phi - \psi(\psi + D_{2,1})(\psi + D_{3,1}) = 0$$
(30a)

This equation contains the six unknown coefficients in \mathbf{p}_{g_2} and \mathbf{p}_{g_3} . Hence, a system of equations obtained from 30a with n=6 values of F will have the same number of equations as unknowns. However, this means it would require one more F value than in Formulation I. To address this, we propose additional equations of the form

$$\mathcal{F}_{1}^{(II)}(\mathbf{p}_{g_{2}},\mathbf{p}_{g_{3}};F_{k}) = \phi(\mathbf{p}_{g_{2}},\mathbf{p}_{g_{3}};F_{k}) - \phi(\mathbf{p}_{g_{2}},\mathbf{p}_{g_{3}};F_{1}) = 0 \quad (30b)$$

which holds at $\mathbf{p}_{g_2}^*$ and $\mathbf{p}_{g_3}^*$ for all F by (29). Using n=5 values of F, the system of equations (30a) and (30b) will consist of 9 equations for 6 unknowns. This requires the same number of F values as in Formulation I, namely n=5. Finally, the coefficient y_0 can be obtained from (28) using $\mathbf{p}_{g_2}^*$ and $\mathbf{p}_{g_3}^*$ without requiring additional data.

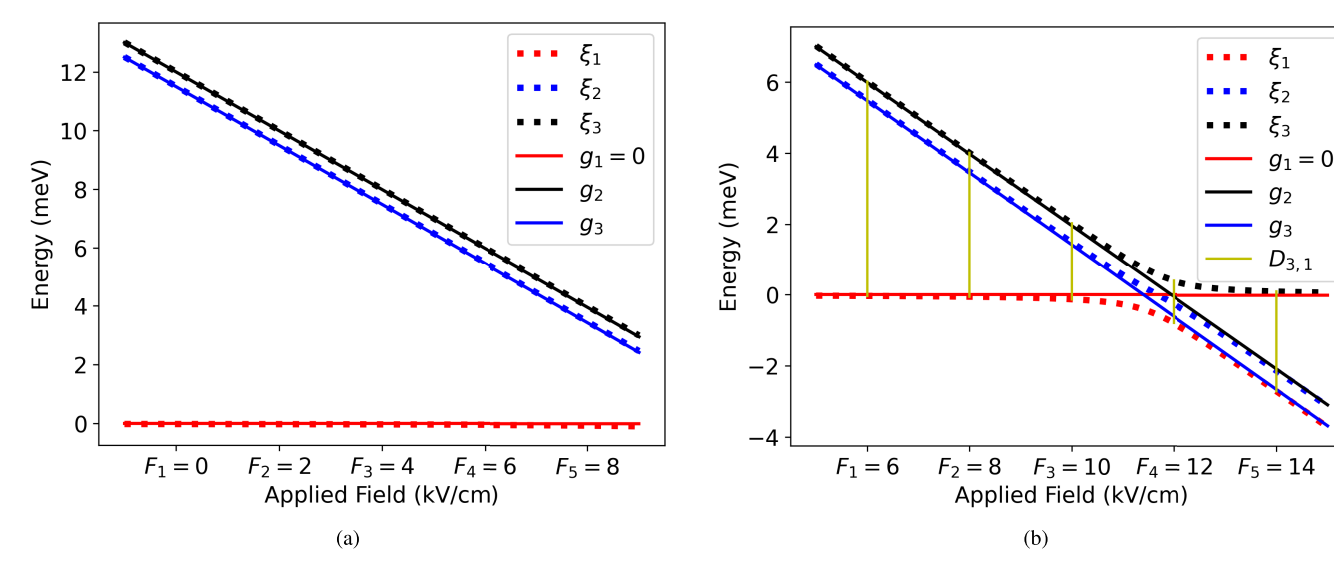


FIGURE 1 | "Asymptotic" relationships between the diagonal elements of G and its eigenvalues. (a) Case I: interval of F away from intersection regions, (b) Case II: the diagonal elements g_1 , g_2 and g_3 intersect near F = 12.

4.2 | Optimization Problem

To recap, Formulation I (27) and Formulation II (30) consist of a system of nonlinear equations for the unknown coefficients, **p**. Given the dataset $M = \{F_k, D_{2,1}(F_k), D_{3,1}(F_k)\}_{k=1}^n$, we propose to solve an ℓ_2 minimization problem for the coefficients **p**. In particular, we aim to solve

minimize
$$L(\mathbf{p}; M) \equiv \sum_{k=1}^{n} \left\{ \left[\mathcal{F}_{0}^{(i)}(\mathbf{p}, F_{k}, D_{2,1}(F_{k}), D_{3,1}(F_{k})) \right]^{2} + \left[\mathcal{F}_{1}^{(i)}(\mathbf{p}, F_{k}, D_{2,1}(F_{k}), D_{3,1}(F_{k})) \right]^{2} \right\}$$
 (31)

where $i \in \{I, II\}$, corresponding to the two different algebraic formulations in Section 4.1. We denote the "true" solution, i.e., the coefficients that generate the dataset M, by \mathbf{p}^* , and the computed solution of the optimization problem by $\tilde{\mathbf{p}}$.

In our numerical experiments, we use a trust-region approach [37], which solves a sequence of constrained subproblems that use quadratic approximations of the objective function. We implemented this approach using the "trust-exact" method in Python's scipy.optimize.minimize package. Similar results were also obtained using line-search methods.

Regardless of the chosen optimization method, good initial iterates are required for convergence to a solution [36]. In what follows we discuss our approach for finding good initial iterates.

4.3 | Warmstarting

Here, we propose approaches for obtaining good initial iterates for the coefficients \mathbf{p} given the dataset M. We recall that the diagonal elements of G are quadratically dependent on F. To describe the main ideas, we consider the following two cases:

Case I: The values of *F* are far from regions where the diagonal elements intersect.

Case II: The values of *F* are near regions where the diagonal elements intersect.

We illustrate these two cases in Figure 1a (Case I) and Figure 1b (Case II).

In Case I, G(F) is diagonally dominant and its eigenvalues are well-approximated by the diagonal elements, that is $\{\xi_1(F), \xi_2(F), \xi_3(F)\}$ are well-approximated by $\{g_1(F) = 0, g_2(F), g_3(F)\}$, for some ordering of the latter. This is illustrated in Figure 1a, where $\xi_1(F) \approx 0, \xi_2(F) \approx g_3(F)$, and $\xi_3(F) \approx g_2(F)$. Therefore, $D_{2,1}(F) \approx g_3(F)$ and $D_{3,1}(F) \approx g_2(F)$. With this in mind, we can compute an initial iterate $\mathbf{p}_{g_2}^{(0)}$ for the coefficients of $g_2(F)$ by choosing $any \ n = 3$ values of F, say F_1 , F_2 , and F_3 , and solving

$$\alpha_2^{(0)} + \beta_2^{(0)} F_1 + \gamma_2^{(0)} F_1^2 = D_{3,1}(F_1)$$
 (32a)

$$\alpha_2^{(0)} + \beta_2^{(0)} F_2 + \gamma_2^{(0)} F_2^2 = D_{3,1}(F_2)$$
 (32b)

$$\alpha_2^{(0)} + \beta_2^{(0)} F_3 + \gamma_2^{(0)} F_3^2 = D_{3,1}(F_3)$$
 (32c)

A similar strategy is used to obtain initial iterates for the coefficients \mathbf{p}_{g_3} of $g_3(F)$ using the same values of F.

In Case II, this strategy needs to be modified. While the eigenvalues can still be approximated by the diagonal elements, the pairings between the $\xi_i(F)$'s and $g_j(F)$'s can vary as a function of F. This is illustrated in Figure 1b, where $g_2(F_1) \approx \xi_3(F_1)$ and $g_2(F_2) \approx \xi_3(F_2)$. However, $g_2(F_5) \approx \xi_2(F_5)$ (not $\xi_3(F_5)$). Furthermore, note that, as in Case I, $\xi_1(F_1)$ and $\xi_1(F_2)$ are approximately zero. However, unlike in Case I, $\xi_3(F_5) \approx 0$. Therefore, to compute an initial iterate $\mathbf{p}_{g_2}^{(0)}$, we solve

$$\alpha_2^{(0)} + \beta_2^{(0)} F_1 + \gamma_2^{(0)} F_1^2 = D_{3,1}(F_1)$$
 (33a)

$$\alpha_2^{(0)} + \beta_2^{(0)} F_2 + \gamma_2^{(0)} F_2^2 = D_{3,1}(F_2) \tag{33b}$$

$$\alpha_2^{(0)} + \beta_2^{(0)} F_5 + \gamma_2^{(0)} F_5^2 = D_{2,1}(F_5) - D_{3,1}(F_5)$$
 (33c)

A similar strategy is used to obtain initial iterates for \mathbf{p}_{g_3} , using the same values of F and its corresponding "asymptotic" pairings.

Note that if we were to investigate a region further to the right of Figure 1b, we would again be "far" from the regions where the diagonal elements intersect, in which case Case I would again be applicable. However, it would differ from Figure 1a in that $\xi_1(F) \approx g_3(F), \xi_2(F) \approx g_2(F)$, and $\xi_3(F) \approx 0$.

To describe this approach in general, we write the system of equations to simultaneously solve for \mathbf{p}_{g_s} and \mathbf{p}_{g_s} as

$$\mathbf{V}_{\sigma}\mathbf{p}_{\sigma}=\mathbf{b}_{\sigma} \tag{34}$$

where

$$\mathbf{V}_{g} = \begin{bmatrix} V & 0 \\ 0 & V \end{bmatrix}, \ \mathbf{p}_{g} = \begin{bmatrix} \mathbf{p}_{g_{2}} \\ \mathbf{p}_{g_{3}} \end{bmatrix}, \text{ and } \mathbf{b}_{g} = \begin{bmatrix} \mathbf{b}_{g_{2}} \\ \mathbf{b}_{g_{3}} \end{bmatrix}$$
 (35)

with $V = V(F_{i_1}, F_{i_2}, F_{i_3})$ a 3×3 Vandermonde matrix with $i_1, i_2, i_3 \in \{1, \dots, n\}$ and the elements of \mathbf{b}_{g_2} and \mathbf{b}_{g_3} correspond to specific "asymptotic" pairing combinations.

In the case where the asymptotics pairings are unknown, we *could* solve (34) for all possible pairings between the eigenvalue and diagonal elements, and use the corresponding solutions as initial iterates to solve (31). However, doing so would require solving the optimization problem many times, each corresponding to a different initialization. To address this more efficiently, we reduce this to a single minimization problem by defining a metric that determines the "best" initial iterate, while using of all n available values of F (in our numerical experiments, n = 5). Let $\mathbf{b}_g[j]$ be as in (35), which here corresponds to the j^{th} pairing between the diagonal elements and eigenvalues. The initial iterate candidate $\mathbf{p}_g^{(0)}[j]$ corresponding to $\mathbf{b}_g[j]$ is given by the solution to the following least squares problem:

$$\mathbf{p}_{g}^{(0)}[j] = \underset{\mathbf{p}_{g} \in \mathbb{R}^{0}}{\min} \ r(\mathbf{p}_{g}) \doteq \|\mathbf{V}_{g}\mathbf{p}_{g} - \mathbf{b}_{g}[j]\|_{2}^{2}$$
 (36)

where \mathbf{V}_g is defined similarly as in (35) but with $V = V(F_1, F_2, \dots, F_n) \in \mathbb{R}^{n \times 3}$. This optimization problem is solved exactly using normal equations. We then compare the squared residuals for all the possible pairings, letting j^* be the index with the smallest squared residual:

$$j^* = \arg\min_{j} \ r\left(\mathbf{p}_g^{(0)}[j]\right) \tag{37}$$

We choose as our initial iterate $\mathbf{p}_g^{(0)} = \mathbf{p}_g^{(0)}[j^*]$. In other words, we choose the initial iterate that is obtained by the pairing that minimizes the two-norm of the residual of (34).

Using these initial iterates, $\mathbf{p}_{g_2}^{(0)}$ and $\mathbf{p}_{g_3}^{(0)}$, an initial iterate for y_0 is obtained from (29). Specifically,

$$y_0^{(0)} = \left[\phi\left(\mathbf{p}_{g_2}^{(0)}, \mathbf{p}_{g_3}^{(0)}; F_k\right)\right]^{1/2},$$

for any F_k , where ϕ is defined in (28).

5 | Numerical Results

We conducted numerical experiments to test the efficacy of the proposed approach outlined in Section 4 using both noiseless and noisy measurements. For the results shown in this section, we used simulated measurement values. These values were created using $\mathbf{p}^* = [y_0, \mathbf{p}_{g_2}, \mathbf{p}_{g_3}]$, where $y_0 = 0.35$, $\mathbf{p}_{g_2} = [12, -1, -0.0008]$, and $\mathbf{p}_{g_3} = [11.5, -1, -0.0004]$, which are similar to values used in previous work [29]. All experiments are conducted using F_1, \ldots, F_5 depicted in Figure 1b.

5.1 | Experiment I: Noiseless Measurements

In the case of noiseless measurements, our approach solves the optimization problem (31) to machine precision when using n = 5 values of F with either Formulation I or II. Figure 2 shows how the loss function (31) converges to zero with iterations for both formulations. However, similar results have been obtained using a variety of selected F values.

To demonstrate this, we create N=30 sets of new coefficients. In particular, these coefficients are defined as

$$\mathbf{q}_{s}^{*} = \Theta_{s} \mathbf{p}^{*}, \quad s = 1, \dots, N$$
(38)

where $\Theta_s \in \mathbb{R}^{7 \times 7}$ is a diagonal matrix with diagonal elements randomly drawn from the interval $[1 - \sigma, 1 + \sigma]$, for some scalar $\sigma > 0$. In this experiment, we use $\sigma = 0.20$.

Table 1 depicts the number of iterations required for each formulation to converge to the solution, given an initial iterate computed using the correct asymptotic pairing. Comparing these formulations, we observe that Formulation II requires fewer iterations on average when the correct asymptotic pairing is used. We surmise that this is due to the "elimination" of y_0 in Formulation II.

To test alternative initial iterates, we also tested using random initial iterates "near" the solution. For each \mathbf{q}_s^* , we generate 10 initial iterates. In particular, these initial iterates are defined as

$$\mathbf{q}_t = \Theta_t \mathbf{q}_s^*, \quad t = 1, \dots, 10 \tag{39}$$

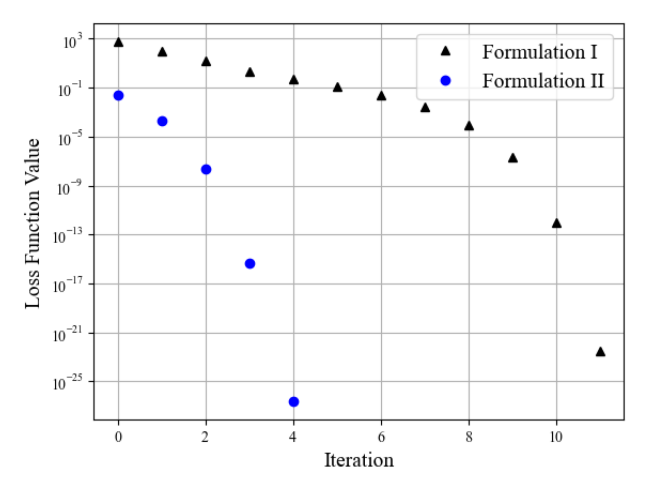


FIGURE 2 | Results for Experiment I: Loss function values using Formulation I and Formulation II as functions of iterations.

 $\Theta_t \in \mathbb{R}^{7 \times 7}$ is a diagonal matrix with diagonal elements randomly drawn from the interval $[1-\rho,1+\rho]$, for some scalar $\rho>0$. In this experiment, we use $\rho=0.20$. As seen in Table 2, the convergence rate for initial iterates with coefficients within $\rho=20\%$ of the true coefficients was just over 80%, versus the 100% observed using the proposed warmstarting method.

5.2 | Experiment II: Noisy Measurements

We model inaccurate measurements and modeling errors as perturbations in the values of the eigenvalue differences. To consider this, we introduce perturbations, $\tau_i(F_k)\epsilon$, at each $D_{i,1}(F_k)$, where $\tau_i(F_k) \in \{-1,1\}$ is a binary random variable and the perturbation parameter ϵ is positive. Thus, we model our noisy eigenvalue differences measurements as

$$\tilde{D}_{i,1}(\epsilon,\tau,F_k) = D_{i,1}(F_k) + \tau_i(F_k)\epsilon \tag{40}$$

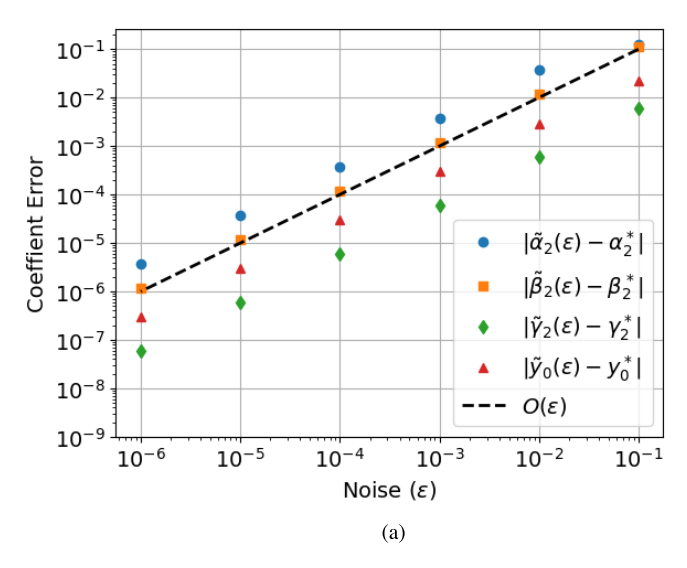
We denote the computed coefficients by $\tilde{\mathbf{p}}(\epsilon)$. To determine the effects of noise on our approach, we simulated noise in the

TABLE 1 | Experiment I: Out of 30 sets of coefficients, this table shows the number of times each formulation converged to a solution using correct initial iterate pairings for various numbers of iterations.

Iterations	4	5	6	7
Formulation I	0	12	14	4
Formulation II	17	8	5	0

TABLE 2 | Experiment I: Out of the 30 sets of coefficients, this table shows the convergence rate to a solution using 10 random initial iterates per set of coefficients versus the proposed warmstart approach.

Initial iterate	Random	Warmstart	
Formulation I	81.33%	100%	
Formulation II	80.67%	100%	



measurements of eigenvalue differences using (40) for six different values of ϵ . In particular, $\epsilon \in \{10^{-1}, \dots, 10^{-6}\}$. As in the first part of Experiment I, we assume that we have the correct asymptotic pairing to initialize the method. Figure 3 depicts the differences between the computed coefficients and the true ones using the two different algebraic formulations. In particular, it illustrates that

$$\|\tilde{\mathbf{p}}(\epsilon) - \mathbf{p}^*\|_2^2 = O(\epsilon) \tag{41}$$

for both formulations. Similar decreases were observed for \mathbf{p}_{g_3} . This shows that our methods are effective in the presence of noise.

5.3 | Experiment III: Warmstart Testing

To test the warmstarting approach, we consider the coefficients sets, \mathbf{q}_s^* , described in Experiment I (see (38)). For each \mathbf{q}_s^* , we repeat Experiment II only using Formulation II, given its better performance than Formulation I for correct asymptotic pairings. However, in this experiment, we obtain initial iterates without assuming knowledge of the correct asymptotic pairings, as described in Section 4.3.

For each new coefficient \mathbf{q}_s^* and perturbation parameter $\epsilon \in \{10^{-1}, \dots, 10^{-6}\}$, we compute the corresponding solution, $\tilde{\mathbf{q}}_s(\epsilon)$, and the maximum error among its coefficients, which is given by

$$\|\tilde{\mathbf{q}}_{s}(\epsilon) - \mathbf{q}_{s}^{*}\|_{\infty}$$
.

These errors are used to calculate the maximum error value

$$\eta(\epsilon) = \max_{s} \|\tilde{\mathbf{q}}_{s}(\epsilon) - \mathbf{q}_{s}^{*}\|_{\infty},$$

and mean error value

$$\mu(\epsilon) = \frac{1}{N} \sum_{s=1}^{N} ||\tilde{\mathbf{q}}_{s}(\epsilon) - \mathbf{q}_{s}^{*}||_{\infty}$$

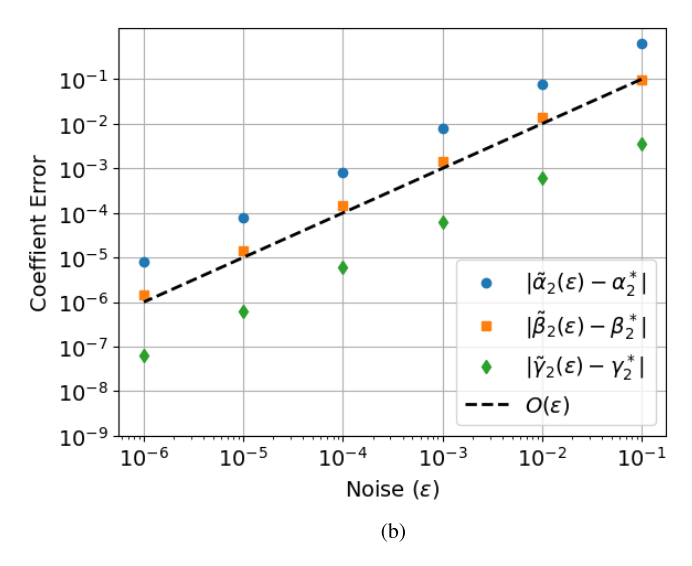


FIGURE 3 | Results of Experiment II. Error in the coefficients y_0 and \mathbf{p}_{g_2} as a function of noise in the data using (a) Formulation I and (b) Formulation II. (a) Coefficient error using Formulation II.

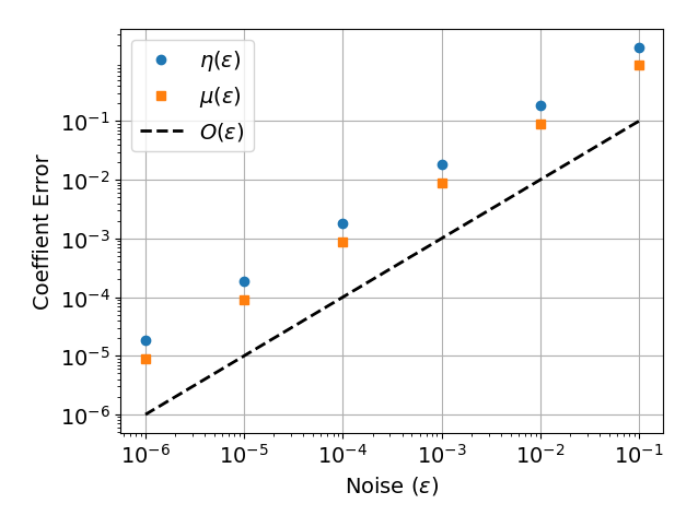


FIGURE 4 | Results of Experiment III: We repeat Experiment II 30 times and report the maximum error value $\eta(\epsilon)$ and mean error value $\mu(\epsilon)$. We only report the results of Formulation II.

for each ϵ . Figure 4 depicts these errors. In particular, it illustrates a decrease of $O(\epsilon)$ in both errors. We conclude from Figure 4 that our optimization approach is effective for solving the IEDP, i.e., minimizing (31), even in the case of unknown asymptotic pairings.

6 | Conclusions

In this article, we formulated the problem to recover the quantum Hamiltonian matrix of a three quantum dot system as a parameterized IEDP. The proposed optimization and warmstarting approach successfully recovers ground state coefficients using eigenvalue differences. In particular, we find that this strategy yields initial iterates, for which the optimization method converges consistently to an accurate solution, even in the presence of noise. Furthermore, the proposed method outperforms random initialization. This demonstrates the feasibility of recovering the physical parameters of a particular three quantum dot system, suggesting extensions to other quantum dot system.

Conflicts of Interest

The authors declare no conflicts of interest.

Data Availability Statement

Data sharing not applicable to this article as no datasets were generated or analysed during the current study.

References

- 1. M. T. Chu, "Inverse Eigenvalue Problems," SIAM Review 40, no. 1 (1998): 1–39.
- 2. M. Chu and G. Golub, *Inverse Eigenvalue Problems: Theory, Algorithms, and Applications* (OUP Oxford, 2005).
- G. Gladwell, Inverse Problems in Vibration (Springer Netherlands, 2005).
- 4. A. Kirsch, An Introduction to the Mathematical Theory of Inverse Problems, vol. 120 (Springer, 2011).

- 5. S. Pirandola, B. R. Bardhan, T. Gehring, C. Weedbrook, and S. Lloyd, "Advances in Photonic Quantum Sensing," *Nature Photonics* 12, no. 12 (2018): 724–733.
- 6. S. Walborn, A. Pimentel, L. Davidovich, and d R. Matos Filho, "Quantum-Enhanced Sensing From Hyperentanglement," *Physical Review A* 97, no. 1 (2018): 010301, https://doi.org/10.1103/PhysRevA.97. 010301.
- 7. B. Stray, A. Lamb, A. Kaushik, et al., "Quantum Sensing for Gravity Cartography," *Nature* 602, no. 7898 (2022): 590–594.
- 8. K. J. Satzinger, Y. Zhong, H. S. Chang, et al., "Quantum Control of Surface Acoustic-Wave Phonons," *Nature* 563, no. 7733 (2018): 661–665, https://doi.org/10.1038/s41586-018-0719-5.
- 9. C. Y. Lai, M. Di Ventra, M. Scheibner, and C. C. Chien, "Tunable Current Circulation in Triangular Quantum-Dot Metastructures," *Europhysics Letters* 123, no. 4 (2018): 47002.
- 10. P. Dugar, M. Scheibner, and C. C. Chien, "Geometry-Based Circulation of Local Photonic Transport in a Triangular Metastructure," *Physical Review A* 102, no. 2 (2020): 23704.
- 11. C. Jennings, X. Ma, T. Wickramasinghe, et al., "Self-Assembled InAs/GaAs Coupled Quantum Dots for Photonic Quantum Technologies," *Advanced Quantum Technologies* 3, no. 2 (2020): 1900085.
- 12. M. Scheibner, A. S. Bracker, D. Kim, and D. Gammon, "Essential Concepts in the Optical Properties of Quantum Dot Molecules," *Solid State Communications* 149, no. 35–36 (2009): 1427–1435.
- 13. A. Vamivakas, Y. Zhao, S. Fält, A. Badolato, J. Taylor, and M. Atatüre, "Nanoscale Optical Electrometer," *Physical Review Letters* 107, no. 16 (2011): 166802.
- 14. S. Ramanathan, G. Petersen, K. Wijesundara, et al., "Quantum-Confined Stark Effects in Coupled InAs/GaAs Quantum Dots," *Applied Physics Letters* 102, no. 21 (2013): 213101, https://doi.org/10.1063/1.4807770.
- 15. H. J. Krenner, M. Sabathil, E. C. Clark, et al., "Direct Observation of Controlled Coupling in an Individual Quantum Dot Molecule," *Physical Review Letters* 94, no. 5 (2005): 057402.
- 16. G. Ortner, M. Bayer, Y. Lyanda-Geller, et al., "Control of Vertically Coupled InGaAs/GaAs Quantum Dots With Electric Fields," *Physical Review Letters* 94, no. 15 (2005): 157401.
- 17. E. A. Stinaff, M. Scheibner, A. S. Bracker, et al., "Optical Signatures of Coupled Quantum Dots," *Science* 311, no. 5761 (2006): 636–639.
- 18. M. Doty, J. Climente, M. Korkusinski, et al., "Antibonding Ground States in InAs Quantum-Dot Molecules," *Physical Review Letters* 102, no. 4 (2009): 047401, https://doi.org/10.1103/PhysRevLett.102.047401.
- 19. M. L. Kerfoot, A. O. Govorov, C. Czarnocki, et al., "Optophononics With Coupled Quantum Dots," *Nature Communications* 5, no. 1 (2014): 3299.
- 20. C. Czarnocki, M. L. Kerfoot, J. Casara, A. R. Jacobs, C. Jennings, and M. Scheibner, "High Resolution Phonon-Assisted Quasi-Resonance Fluorescence Spectroscopy," *Journal of Visualized Experiments: Jove* 112 (2016): 53719.
- 21. J. Seufert, M. Obert, M. Scheibner, et al., "Stark Effect and Polarizability in a Single CdSe/ZnSe Quantum Dot," *Applied Physics Letters* 79, no. 7 (2001): 1033–1035.
- 22. A. S. Bracker, M. Scheibner, M. Doty, et al., "Engineering Electron and Hole Tunneling With Asymmetric InAs Quantum Dot Molecules," *Applied Physics Letters* 89, no. 23 (2006): 233110, https://doi.org/10.1063/1.2400397.
- 23. M. Scheibner, M. Yakes, A. S. Bracker, et al., "Optically Mapping the Electronic Structure of Coupled Quantum Dots," *Nature Physics* 4, no. 4 (2008): 291–295.

- 24. M. T. Chu and G. H. Golub, "Structured Inverse Eigenvalue Problems," *Acta Numerica* 11 (2002): 1–71.
- 25. H. Dai, Z. Z. Bai, and Y. Wei, "On the Solvability Condition and Numerical Algorithm for the Parameterized Generalized Inverse Eigenvalue Problem," *SIAM Journal on Matrix Analysis and Applications* 36, no. 2 (2015): 707–726, https://doi.org/10.1137/140972494.
- 26. S. L. J. Hu and H. Li, "A Systematic Linear Space Approach to Solving Partially Described Inverse Eigenvalue Problems," *Inverse Problems* 24, no. 3 (2008): 035014, https://doi.org/10.1088/0266-5611/24/3/035014.
- 27. Z. J. Bai, S. Serra-Capizzano, and Z. Zhao, "Nonnegative Inverse Eigenvalue Problems With Partial Eigendata," *Numerische Mathematik* 120, no. 3 (2012): 387–431.
- 28. M. Scheibner, M. Doty, I. V. Ponomarev, et al., "Spin Fine Structure of Optically Excited Quantum Dot Molecules," *Physical Review B* 75, no. 24 (2007): 245318, https://doi.org/10.1103/PhysRevB.75.245318.
- 29. K. Wright, R. Marcia, M. Scheibner, and B. Ilan, "Parameterized Inverse Eigenvalue Problem for Quantum Sensing," in 2023 IEEE 9th International Workshop on Computational Advances in Multi-Sensor Adaptive Processing (CAMSAP) (IEEE, 2023), 351–355.
- 30. N. Wagner, "Inverse Eigenvalue Problems in Structural Dynamics," *Pammatone* 6, no. 1 (2006): 339–340, https://doi.org/10.1002/pamm. 200610151.
- 31. H. Dai and P. Lancaster, "Newton's Method for a Generalized Inverse Eigenvalue Problem," *Numerical Linear Algebra With Applications* 4, no. 1 (1997): 1–21.
- 32. S. Friedland, J. Nocedal, and M. L. Overton, "The Formulation and Analysis of Numerical Methods for Inverse Eigenvalue Problems," *SIAM Journal on Numerical Analysis* 24, no. 3 (1987): 634–667.
- 33. J. D. Mar, J. J. Baumberg, X. L. Xu, A. C. Irvine, and D. A. Williams, "Precise Measurements of the Dipole Moment and Polarizability of the Neutral Exciton and Positive Trion in a Single Quantum Dot," *Physical Review B* 95 (2017): 201304, https://doi.org/10.1103/PhysRevB.95.201304.
- 34. H. Cohen, "Resultants and Discriminants," in *A Course in Computational Algebraic Number Theory* (Springer Verlag, 1993).
- 35. I. M. Gelfand, M. M. Kapranov, and A. V. Zelevinsky, *Discriminants and Resultants for Polynomials in One Variable* (Birkhäuser Boston, 1994), 397–425.
- 36. K. Wright, R. Marcia, and B. Ilan, "Numerical Methods for a Schrödinger Equation Inverse Eigenvalue Problem," in 15th International Conference on Mathematical and Numerical Aspects of Wave Propagation Waves (ENSTA-Paris, 2022).
- 37. A. R. Conn, N. I. Gould, and P. L. Toint, *Trust-Region Methods* (SIAM, 2000).

Appendix A

The (1,1) Entry of G(F)

We now demonstrate that, for our IEDP, without loss of generality, one can set the (1,1) element of G(F) to zero, i.e., $g_1(F)=0$ in (1).

Consider the shifted matrix

$$\tilde{G}(F) = G(F) + \delta(F)I \tag{A1}$$

where $\delta(F)$ is any scalar-valued function of F and I is the identity matrix. Let $\{\tilde{\xi}_1(F), \tilde{\xi}_2(F), \tilde{\xi}_3(F)\}$ be the eigenvalues of $\tilde{G}(F)$, with $\tilde{\xi}_1(F) \leq \tilde{\xi}_2(F) \leq \tilde{\xi}_3(F)$. Note that $\tilde{\xi}_i(F) = \xi_i(F) + \delta(F)$ for i = 1, 2, 3. Then the eigenvalue differences in $\tilde{G}(F)$ are equal to the eigenvalue differences in G(F) since

$$\tilde{\xi}_i(F) - \tilde{\xi}_j(F) = (\xi_i(F) + \delta(F)) - (\xi_j(F) + \delta(F)) = \xi_i(F) - \xi_j(F) \quad (A2)$$

for all i and j. Thus, if G(F) is a solution to our IEDP, then so is $\tilde{G}(F)$. Choosing $\delta(F) = -g_1(F)$ yields a solution whose (1,1) is zero. Thus, without loss of generality, we may set $g_1(F) = 0$.

Appendix B

Proof of Proposition 1

Proof. The proof consists of the following parts: (1)The same eigenvalue differences can be obtained using $\{\xi_1, \xi_2, \xi_3\}$ or $\{-\xi_3, -\xi_2, -\xi_1\}$. (2) Given a set of eigenvalues and a solution with g_2 and g_3 , then another solution exists by swapping g_2 and g_3 . (3) Given a set of eigenvalues, no other solutions can be obtained using five or more values of F. (4) Given a set of eigenvalue differences and a solution with g_2 and g_3 , then another solution exists with $-g_2$ and $-g_3$. (5) Given a set of eigenvalue differences and a solution with g_3 and g_2 , then another solution exists with $-g_3$ and $-g_2$. (6) Given the set of eigenvalue differences, no other solutions exist.

1. We first identify that there are two possible sets of eigenvalues for G defined in (8) that both satisfy a set of eigenvalue differences, $\{D_{3,1}, D_{2,1}, D_{3,2}\}$ and maintain $g_1(F) \equiv 0$, namely,

$$\{\xi_1, \xi_2, \xi_3\}$$
 and $\{-\xi_3, -\xi_2, -\xi_1\}$ (B1)

The first set satisfies the eigenvalue differences by definition. Since the eigenvalues are defined in increasing order, let $\hat{\xi}_3 = -\xi_1$, $\hat{\xi}_2 = -\xi_2$, and $\hat{\xi}_1 = -\xi_3$, where $\hat{\xi}_3 \geq \hat{\xi}_1 \geq \hat{\xi}_1$. Using $\hat{D}_{2,1}$, $\hat{D}_{3,1}$, and $\hat{D}_{3,2}$ as defined similarly in (4–6), by substitution we have that

$$\hat{D}_{2,1}(F) = -\xi_2(F) - (-\xi_3(F)) = D_{3,2}, \tag{B2}$$

$$\hat{D}_{3,1}(F) = -\xi_1(F) - (-\xi_3(F)) = D_{3,1}, \tag{B3}$$

$$\hat{D}_{3,2}(F) = -\xi_1(F) - (-\xi_2(F)) = D_{2,1}, \tag{B4}$$

which shows $\{\hat{D}_{3,1}, \hat{D}_{2,1}, \hat{D}_{3,2}\} = \{D_{3,1}, D_{2,1}, D_{3,2}\}.$

- **2.** The fact that $[y_0^*, \mathbf{p}_{g_3}^*, \mathbf{p}_{g_2}^*]$ is also a solution follows from swapping the second and third rows and columns of the *G* matrix (8).
- **3.** We now demonstrate that, given the eigenvalue set $\{\xi_1,\xi_2,\xi_3\}$ and solutions $[y_0^*,\mathbf{p}_{g_3}^*,\mathbf{p}_{g_3}^*]$ and $[y_0^*,\mathbf{p}_{g_3}^*,\mathbf{p}_{g_3}^*]$, no additional solutions exist.

Lemma 1. Suppose $[y_0^*, \mathbf{p}_{g_2}^*, \mathbf{p}_{g_3}^*]$ and $[y_0^*, \mathbf{p}_{g_3}^*, \mathbf{p}_{g_2}^*]$ are solutions to the IEDP with eigenvalues $\{\xi_1, \xi_2, \xi_3\}$ for $F \in \{F_1, \ldots, F_5\}$. Suppose there is an additional solution

$$\mathbf{q}^* = [y_0^*, \mathbf{q}_{h_*}^*, \mathbf{q}_{h_*}^*] \tag{B5}$$

where $\mathbf{q}_{h_2}^* = [a_2^*, b_2^*, c_2^*]$ and $\mathbf{q}_{h_3}^* = [a_3^*, b_3^*, c_3^*]$, which correspond to the quadratic polynomials

$$h_i(F) = a_i^* + b_i^* F + c_i^* F^2, \quad i = 2, 3.$$
 (B6)

Then, \mathbf{q}^* is of the form $[y_0^*, \mathbf{p}_{g_2}^*, \mathbf{p}_{g_3}^*]$ or $[y_0^*, \mathbf{p}_{g_3}^*, \mathbf{p}_{g_2}^*]$.

Proof. First, we rewrite (22) as an equivalent system (see [29]) of the form

$$-y_0^2(\xi_1 + \xi_2 + \xi_3) - \xi_1 \xi_2 \xi_3 = 0$$
 (B7a)

$$g_2^2 + g_2(\xi_1 + \xi_2 + \xi_3) + 2y_0^2 + \xi_1\xi_2 + \xi_1\xi_3 + \xi_2\xi_3 = 0$$
 (B7b)

$$g_2 + g_3 - \xi_1 - \xi_2 - \xi_3 = 0 (B7c)$$

where $g_j(F) = \alpha_j + \beta_j F + \gamma_j F^2$ for j = 2, 3. Solving this system yields

$$y_0 = \pm \sqrt{-\frac{\xi_1 \xi_2 \xi_3}{\xi_1 + \xi_2 + \xi_3}}$$
 (B8a)

$$\begin{split} g_2^{\pm} &= \frac{1}{2} (\xi_1 + \xi_2 + \xi_3) \\ &\pm \frac{\sqrt{(\xi_1 - \xi_2 - \xi_3)(\xi_1 - \xi_2 + \xi_3)(\xi_1 + \xi_2 - \xi_3)(\xi_1 + \xi_2 + \xi_3)}}{2(\xi_1 + \xi_2 + \xi_3)} \quad \text{(B8b)} \end{split}$$

$$\begin{split} g_3^{\mp} &= \frac{1}{2} (\xi_1 + \xi_2 + \xi_3) \\ &\mp \frac{\sqrt{(\xi_1 - \xi_2 - \xi_3)(\xi_1 - \xi_2 + \xi_3)(\xi_1 + \xi_2 - \xi_3)(\xi_1 + \xi_2 + \xi_3)}}{2(\xi_1 + \xi_2 + \xi_3)} \end{split} \tag{B8c}$$

where the superscript "+" corresponds to the positive root and the superscript "-" corresponds to the negative root. It follows from (B8a) that we have two sets of solutions, each corresponding to a sign of y_0 . However, we only consider the case where $y_0 > 0$. Note from (B8b) and (B8c) that $g_2^{\pm} = g_3^{\pm}$. Using these notations, if $g_2 = g_2^{+} = g_3^{+}$, then $g_3 = g_3^{-} = g_2^{-}$. Alternatively, if $g_2 = g_2^{-} = g_3^{-}$, then $g_3 = g_3^{+} = g_2^{+}$. This yields the two solutions $[y_0^*, \mathbf{p}_{g_1}^*, \mathbf{p}_{g_2}^*]$ and $[y_0^*, \mathbf{p}_{g_3}^*, \mathbf{p}_{g_3}^*]$.

Without loss of generality, we assume that $g_2(F) = g_2^+(F)$ in (B8b) and $g_3(F) = g_3^-(F)$ in (B8c). Note that by their definition, $h_2(F)$ and $h_3(F)$ must also satisfy (B8b) and (B8c), respectively, at each F_k ($k = 1, \ldots, n$). Thus, for \mathbf{q}^* to be a solution, it must satisfy, at each F_k ,

$$h_2(F_k) = g_2(F_k)$$
 and $h_3(F_k) = g_3(F_k)$ (B9a)

or

$$h_2(F_k) = g_3(F_k)$$
 and $h_3(F_k) = g_2(F_k)$ (B9b)

For $n \ge 5$, (B9a) or (B9b) (or both) must hold for at least three values of F. If (B9a) holds for at least three values of F, then $h_2(F) \equiv g_2(F)$ and $h_3(F) \equiv g_3(F)$ since they are quadratic polynomials that intersect at least three different points. Hence, $\mathbf{q}_{h_2}^* = \mathbf{p}_{g_2}^*$ and $\mathbf{q}_{h_3}^* = \mathbf{p}_{g_3}^*$. Similarly, if (B9b) holds for at least three values of F, then $h_2(F) \equiv g_3(F)$ and $h_3(F) \equiv g_2(F)$. Hence, $\mathbf{q}_{h_2}^* = \mathbf{p}_{g_3}^*$ and $\mathbf{q}_{h_3}^* = \mathbf{p}_{g_2}^*$. Thus, \mathbf{q}^* is of the form $[y_0^*, \mathbf{p}_{g_2}^*, \mathbf{p}_{g_3}^*]$ or $[y_0^*, \mathbf{p}_{g_2}^*, \mathbf{p}_{g_3}^*]$.

From Lemma (1), given the eigenvalue set $\{\xi_1, \xi_2, \xi_3\}$, no additional solutions exist.

4. We now demonstrate that if $[y_0^*, \mathbf{p}_{g_2}^*, \mathbf{p}_{g_3}^*]$ is a solution to the IEDP corresponding to the eigenvalue set $\{\xi_1, \xi_2, \xi_3\}$, then $[y_0^*, -\mathbf{p}_{g_3}^*, -\mathbf{p}_{g_3}^*]$ is a solution to the IEDP corresponding to the eigenvalue set $\{-\xi_3, -\xi_2, -\xi_1\}$.

Lemma 2. If $[y_0^*, \mathbf{p}_{g_3}^*, \mathbf{p}_{g_3}^*]$ is a solution to the IEDP corresponding to the eigenvalue set $\{\xi_1, \xi_2, \xi_3\}$, then $[y_0^*, -\mathbf{p}_{g_2}^*, -\mathbf{p}_{g_3}^*]$ is a solution to the IEDP corresponding to the eigenvalue set $\{-\xi_3, -\xi_2, -\xi_1\}$.

Proof. Given $[y_0^*, \mathbf{p}_{g_2}^*, \mathbf{p}_{g_3}^*]$ is a solution to the IEDP using the eigenvalue set $\{\xi_1, \xi_2, \xi_3\}$, the matrix

$$-G(F) = \begin{bmatrix} 0 & -y_0 & -y_0 \\ -y_0 & -g_2(F) & 0 \\ -y_0 & 0 & -g_3(F) \end{bmatrix}$$
(B10)

also satisfies the eigenvalue differences with eigenvalues $\{-\xi_3, -\xi_2, -\xi_1\}$, but is not a solution since $-y_0 < 0$. Pre- and post-multiplying -G by the 3×3 diagonal matrix $P = \mathrm{diag}\,(1, -1, -1)$ yields

$$\hat{G} = P(-G)P = \begin{bmatrix} 0 & y_0 & y_0 \\ y_0 & -g_2(F) & 0 \\ y_0 & 0 & -g_3(F) \end{bmatrix}$$
(B11)

Note that $P = P^{-1}$. Therefore, \hat{G} is similar to -G and consequently has the same eigenvalues as -G, which has the same eigenvalue differences as G. Therefore, $[y_0^*, -\mathbf{p}_{g_2}^*, -\mathbf{p}_{g_3}^*]$ is a solution.

From Lemma (2), since $[y_0^*, \mathbf{p}_{g_2}^*, \mathbf{p}_{g_3}^*]$ is a solution to the IEDP, then $[y_0^*, -\mathbf{p}_{g_3}^*, -\mathbf{p}_{g_3}^*]$ is also a solution to the IEDP.

- **5.** Similarly to Part 4, from Lemma (2), since $[y_0^*, \mathbf{p}_{g_3}^*, \mathbf{p}_{g_2}^*]$ is a solution to the IEDP, then $[y_0^*, -\mathbf{p}_{g_3}^*, -\mathbf{p}_{g_3}^*]$ is also a solution to the IEDP.
- 6. Given the two solutions to the IEDP

$$[y_0^*, -\mathbf{p}_{g_0}^*, -\mathbf{p}_{g_2}^*]$$
 and $[y_0^*, -\mathbf{p}_{g_0}^*, -\mathbf{p}_{g_2}^*]$ (B12)

corresponding to $\{-\xi_3, -\xi_2, -\xi_1\}$, then no additional solutions exist corresponding to $\{-\xi_3, -\xi_2, -\xi_1\}$ per Lemma (1).

Thus, the four solutions to the IEDP are

$$[y_0^*, \mathbf{p}_{g_2}^*, \mathbf{p}_{g_3}^*], \quad [y_0^*, \mathbf{p}_{g_3}^*, \mathbf{p}_{g_2}^*], \quad [y_0^*, -\mathbf{p}_{g_2}^*, -\mathbf{p}_{g_3}^*], \quad \text{and}$$

$$[y_0^*, -\mathbf{p}_{g_3}^*, -\mathbf{p}_{g_3}^*]$$
 (B13)

concluding the proof.